Imine based self-healing hydrogel triggered by periodate

*Alexis Wolfel, Cecilia Inés Alvarez Igarzabal, and Marcelo R. Romero**

Laboratorio de Materiales Poliméricos (LAMAP), Departamento de Química Orgánica, Universidad Nacional de Córdoba, Instituto Investigación en Ingeniería de Procesos y Química Aplicada (IPQA-CONICET), Haya de la Torre y Medina Allende, Córdoba, Argentina.

**marceloricardoromero@gmail.com*

Phone: (54) 0351-5353867/69

GRAPHICAL ABSTRACT

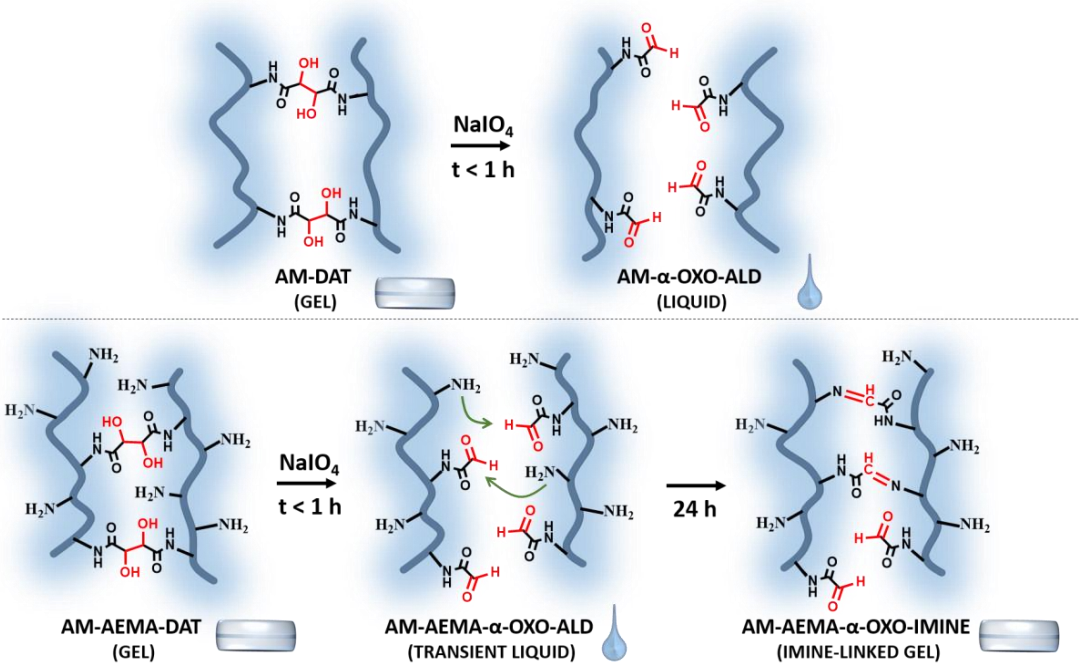

ABSTRACT

The development of new materials with smart properties is currently expanding the development of new technologies. Therefore, the design of materials with novel sensitivities and smart behavior is important for the development of smart systems with automated responsivity. We have recently reported the synthesis of hydrogels, cross-linked by *N,N'*-diallyltartardiamide (DAT). The covalent DAT-crosslinking points have vicinal diols which can be easily cleaved with periodate, generating changes in the hydrogel properties, as well as generating valuable α-oxo-aldehyde functional groups useful for further chemical modification. Based on those findings, we envisioned that a self-healable hydrogel could be obtained by incorporation of primary amino functional groups, from 2-aminoethyl methacrylate hydrochloride (AEMA), coexisting with DAT into the same network. Herein, α-oxo-aldehyde groups generated after the reaction with periodate would arise in the immediate environment of amine groups to form imine cross-links. For this purpose, DAT-crosslinked hydrogels were synthesized and carefully characterized. The cleavage of DAT-crosslinks with periodate promoted changes in the mechanical and swelling properties of the materials. As expected, a self-healing behavior was observed, based on the spontaneous formation of imine covalent bonds. In addition, we surprisingly found a combination of fast vicinal diols cleavage and a low speed self-crosslinking reaction by imine formation. Consequently, it was found a time-window in which a periodate-treated polymer was obtained in a transient liquid state, which can be exploited to choose the final shape of the material, before automated gelling. The singular properties attained on these hydrogels could be useful for developing sensors, actuators, among other smart systems.

Keywords: self-healing, imine, Schiff base, periodate, diol, *N,N'*-diallyltartardiamide, α-oxoaldehyde, 2-aminoethyl methacrylate

1. INTRODUCTION

Smart hydrogels (HGs) can change their properties in a functional and predictable manner in response to external stimuli.[1] This stimuli-responsive behavior expanded their potential applications by the amplification of their sensitivity to a wide range of stimulus, and promoting different smart-responsiveness such as: sol-gel transitions, volume phase transitions; changes on the mechanical or swelling properties, or in the color, modifications on their conductivity, among others.[2] During the last decade, a new generation of smart-materials gained much attention showing advanced properties such as self-healing and shape memory.[2,3] In HGs, these properties are usually achieved by a combination of stable and dynamic bonds (secondary, covalent, or supramolecular), which can generate new linkages upon an external damage and/or triggered by an external stimulus, to repair the material, and/or to recover a predefined shape.[4] Moreover, for some self-healing materials, the curing ability can be selectively triggered by environmental stimulus (non-autonomic self-healing) such as changes in: moisture content[5]; pH[6]; UV-light[7]; among others[8]; which can be useful for particular applications such as tissue engineering[9] or 3D-printing[8].

In particular, the adaptability of strong interactions such as covalent bonds, modifying the molecular architecture of materials in response to external stimuli, is one of the current challenges.[10,11] These bonds can improve the ability of materials to withstand mechanical stress and also provide intelligent properties for uses as sensors/actuators, *in-situ* gelling materials, tissue engineering, controlled-release of bioactive drugs,

among others.[4,10,12,13] In this respect, imine bonds ($RN=CR_2$; with R = H and / or hydrocarbyl) are formed by reaction of an amino functional group (FG) with a ketone or an aldehyde, and usually show a reversible behavior in aqueous solution.[14] The reversible imine bond formation/hydrolysis is highly dependent on the environmental conditions and the chemical nature of the participant molecules.[15] Furthermore, imine formation is usually achieved with high selectivity and specificity at physiological conditions, and is then widely used for bioconjugation.[16,17] Moreover, this bonds have been exploited for the development of HGs with self-healing[18,19] and shape memory[20] properties; injectable type[21], with the possibility of releasing drugs in a controlled manner[22]; among others. However, the incorporation of imine cross-links into HGs based on vinylic monomers usually involves the difficulty of obtain the reactive precursors into the network. Whereas amine FGs can be easily obtained by incorporating amino vinylic monomers, on the contrary, the aldehyde functionalization represents a challenge. Aldehyde bearing monomers are usually toxic and unstable under polymerization conditions, making necessary to protect the aldehyde FG.[23]Typically, this procedure involves several reaction steps to introduce and remove the protecting groups. As a straight forward protocol, we have previously demonstrated the use of an effortless post-synthesis modification of the cross-linker *N,N'*-diallyltartardiamide (DAT) to obtain valuable α-oxoaldehyde FGs.[24] This modification is promoted by the periodate-mediated cleavage of diol FGs, a quick reaction that is mild enough to be used on living cells.[25–27] The combination of those α-oxoaldehyde groups with amino FGs into hydrogel networks, could open a window for an easy yield of chemoselective imine covalent linkages in HGs. The reactivity of α-oxo-aldehyde with

amine groups in synthetic polymers, only has scarce antecedents in which DAT cross-linker was used for immobilization of ligands in polymeric matrices by reductive amination.[28–30] The coexistence of α-oxo-aldehyde with amino FGs in polymeric networks, to generate imine as cross-linking points, could give rise to materials with properties such as shape memory, sol-gel transitions and self-healing. Furthermore, the chemoselectivity of imine bond formation could enable the gelation under physiological conditions and the immobilization of biomolecules and/or drugs for biomedical applications.[31]

As previously mentioned, amino FGs can be included by free radical polymerization of vinyl monomers such as 2-aminoethyl methacrylate monomer (AEMA). The homopolymer poly-(2-aminoethyl methacrylate) (p-AEMA) and its copolymer with *N,N'*-methylenebis(acrylamide) (BIS) have proven biocompatibility.[32,33] In addition, the amino FG introduced by AEMA have been used to include useful modifications on different materials. In some cases, it was used for conjugation with aldehyde or ketone FGs through the formation of imines. For example, for the immobilization of functional molecules into synthetic polymers, for applications such as antifungal materials[34]; waste water treatment[35]; or development of polymeric inks[36].

In line with the above considerations, herein we propose the obtainment of self-healing HGs based on acrylamide (AM) and AEMA, covalently cross-linked with DAT, alone or together with BIS. After the characterization of the effects caused by the incorporation of DAT and AEMA, the HGs were treated with an aqueous solution of sodium periodate, at room temperature, to broke DAT-crosslinks and yield aldehyde pendant groups. Then, a self-healing process was observed in the hydrogels, caused by the formation of new

imine bonds. The automatic reparation of the network demonstrated the potential of this chemical strategy for the yield of covalently bonded self-healing materials which could be useful in several applications.

2. MATERIALS AND METHODS

2.1 Reagents

For the synthesis of HGs, acrylamide (AM), 2-aminoethylmethacrylate hydrochloride (AEMA), and both cross-linking agents, (+)-*N,N′*-diallyltartardiamide (DAT) and *N,N′*-methylenebisacrylamide (BIS) (Figure 1) (*Aldrich*), were used. The polymerization reaction was initiated with ammonium persulfate (APS) (*Anedra*), and the activator *N,N,N′,N’*-tetramethylethylenediamine (TEMED) (*Aldrich*). The HGs were modified with sodium periodate ($NaIO_4$) (*Aldrich*). Picryl sulfonic acid (TNBS) (*Sigma*), in a concentration of 5% (w/v) in H_2O, was used for the identification test of amine groups. All the reagents were used as received. The solutions were prepared with ultra-pure water ($18M\Omega cm^{-1}$).

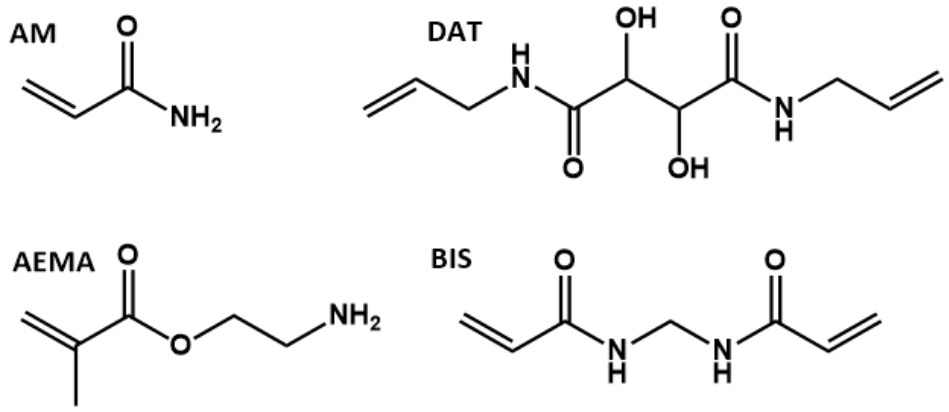

Figure 1. Reagents used in the synthesis of hydrogels (HGs).

2.2 SYNTHESIS

The HGs were prepared by free radical polymerization. For this, the monomers AM:AEMA in a molar ratio of 95:5 (7 mmol in total), different quantities of cross-linking agents (see Table 1) and APS (0.26 mmol) were dissolved in ultrapure water to a final volume of 5 mL, in a vial with a rubber cap. Then, each solution was cooled in an ice water bath and deoxygenated by bubbling N_2 for 10 min. To start the polymerization, 0.5 mL of a TEMED solution (0.32 M) was added to the vial, and each solution was transferred to 5 mL disposable syringes. The syringes were placed in a thermal water bath at 50 °C for 16 h. Finally, the HGs were cut into discs of 3 mm thick and 12 mm in diameter and washed thoroughly with water.

Table 1. Composition of the synthesized HGs.

Nomenclature	***AM:AEMA mol ratio***	***Cross-linkers (%)****
p-AM-AEMA-BIS	**95:5**	**BIS (5) - DAT (0)**
p-AM-AEMA-BIS-DAT(1)	**95:5**	**BIS (5) - DAT (1)**
p-AM-AEMA-BIS-DAT(3)	**95:5**	**BIS (5) - DAT (3)**
p-AM-AEMA-BIS-DAT(5)	**95:5**	**BIS (5) - DAT (5)**
p-AM-AEMA-BIS-DAT(7)	**95:5**	**BIS (5) - DAT (7)**
p-AM-AEMA-BIS-DAT(10)	**95:5**	**BIS (5) - DAT (10)**
p-AM-BIS-DAT(10)	**100:0**	**BIS (5) - DAT (10)**
p-AM-AEMA-DAT(10)	**95:5**	**BIS (0) - DAT (10)**
p-AM-DAT(10)	**100:0**	**BIS (0) - DAT (10)**

***Molar percentage with respect to total moles of monomers.**

2.3 POST-SYNTHETIC MODIFICATION OF HGs

2.3.1 Treatment of p-AM-AEMA-BIS-DAT with periodate

The HG discs were dried in an oven at 37 ºC (≈ 80 mg of dried mass). Then, they were swelled in 50 mL of water for 3 days. Once attained equilibrium, they were placed in vials containing 1.5 mL of 0.2 M sodium periodate solution and stirred in an orbital oscillator for 1 h. The reaction was quenched by adding 2 mL of 4 % v/v glycerol solution. Then, the discs were thoroughly washed with distilled water. For swelling rate measurements (SR, see Section 2.4.1) during the reaction, a similar procedure was followed, without the addition of glycerol; the mass was measured every hour gravimetrically.

2.3.2 Total degradation of cross-links and gel self-healing

HGs synthesized using only DAT as a cross-linker (p-AM-DAT and p-AM-AEMA-DAT, see Table 1) were submitted to total degradation of their cross-links. Previously, the dried gel discs (≈ 80 mg of dried mass) were swelled to equilibrium in water, and placed in vials. To perform the total degradation, 1.25 mL of 0.1 M $NaIO_4$ solution was added, estimating excess of the oxidant. Then, the self-curing behavior of the fully degraded products was analyzed. The total degradation phenomenon was filmed and processed with the mobile application “Framelapse” [Singh, N. (2017), Framelapse - Time Lapse Camera (4.1) - Mobile application software. Retrieved from https://play.google.com/store/apps/details?id=com.Nishant.Singh.DroidTimelapse].

2.3.3 Amine detection by a coloration test with TNBS

For the identification of amino groups, pieces of the different HGs (about 50 mg of swollen mass) fully swollen in water, were immersed into 1 mL of saturated solution of sodium borate for 1 h. Subsequently, 90 µL of 1.5 % w/v TNBS solution in ethanol was added. After 3 h, photographs of the tested materials were recorded.

2.4 CHARACTERIZATION OF THE HGs

2.4.1 Swelling studies

The HGs discs (≈ 80 mg of dried mass) were swollen in distilled water (250 mL) in a beaker, at 20 °C for three days, until reaching constant mass. The mass of the dehydrated products was obtained by drying the discs in an oven at 37 °C until constant weight.

The equilibrium swelling ratio (ESR) was calculated according to Equation 1.[37]

$$ESR = (m_e - m_s) / m_s \quad \text{(Equation 1)}$$

Where $\mathbf{m_e}$ is the mass of the gel in its swelling equilibrium, and $\mathbf{m_s}$ corresponds to the mass of dry hydrogel.

The swelling kinetic of the HGs was studied by determining the swelling rate (SR) at different times. To perform this study, the dehydrated discs (≈ 80 mg of dried mass) were submerged in water (250 mL) in a beaker, and the weight changes were recorded as a function of time, until a constant mass was reached. The SR was calculated using Equation 2, where $\mathbf{m_t}$ corresponds to the gel mass at a certain time [14]:

$$SR = (m_t - m_s) / m_s \quad \text{(Equation 2)}$$

Based on the swelling kinetic of the HGs, the type of water diffusion within the matrix was estimated using the Equation 3:

$$M_t / M_\infty = vt^n \quad \text{(Equation 3)}$$

Where $\mathbf{M_t}$ corresponds to the mass of water incorporated into the sample at time **t**; $\mathbf{M_\infty}$ is the mass of water incorporated into the gel at equilibrium, and v is a constant related to the structure of the network. The exponent **n** is a number related to the type of diffusion. This equation is applicable only during the onset of swelling, when it is less than 60% of equilibrium. The value of **n** and **v** were obtained from the slope and intercept of the curve *ln* ($\mathbf{M_t}$ */* $\mathbf{M_\infty}$) vs. *ln* **t**.[37]

2.4.2 Infrared spectroscopy (FT-IR) and nuclear magnetic resonance (NMR)

The samples were analyzed by infrared spectroscopy (FT-IR) in a Nicolet 5-SXC FTIR Spectrometer. Discs were prepared by mixing about 2 mg of xerogel or dehydrated monomer and 100 mg of KBr. The mixture was pulverized in a mortar and then compacted into a thin disk using a 10 Ton hydraulic press. The FT-IR spectra were acquired in the spectral range of 4000-400 cm^{-1} with a resolution of 4 cm^{-1} using 64 scans per sample.

The ^{1}H-NMR and ^{13}C-NMR spectra were obtained on a 400 MHz Bruker Advance Nuclear Magnetic Resonance Spectrometer (USA) using dried and ground samples, subsequently swollen in D_2O.

3. RESULTS AND DISCUSSION

Copolymers of acrylamide (AM) and 2-aminoethyl methacrylate (AEMA) cross-linked in absence or presence of BIS (5 mol%, respect to total moles of monomers) and different DAT amounts (0; 1; 3; 5; 7 and 10 mol%) were synthesized, as indicated in Table 1. In all cases, HGs with good mechanical properties, easy to handle without generating visible damages, were obtained.

We have previously reported the synthesis of AM-BIS-DAT HGs where the periodate mediated cleavage of DAT-crosslinks caused the formation of aldehyde FGs in the network.[24] In this work, we aimed to enhance their smart properties by incorporating an imine based self-healing behavior which could be triggered by periodate. Thus, AEMA incorporation was needed for obtaining amines in the network, that would later be combined with the aldehyde FGs that could be formed by the presence of periodate. However, AEMA incorporation could modify the delicate balance which controls the swelling equilibrium of HGs, by affecting the hydrophilicity of the polymers, the interactions between polymer chains (covalent or non-covalent) or even the reactivity of the system during polymerization conditions. Therefore, swelling studies were performed to verify the effect of using different amounts of cross-linker DAT in the equilibrium swelling rate (ESR) of the HGs containing AEMA (AM-AEMA-BIS-DAT), and were compared with those in absence of AEMA (AM-BIS-DAT) (Figure 2). In general, the marked decrease in ESR with the increase in %DAT (Figure 2A) evidenced an efficient incorporation of a greater number of covalent cross-links in both systems. These cross-links act as "knots" between network chains, limiting the capacity of expansion of the gel and restricting the absorption of higher volumes of solvent. However, AEMA containing networks showed a reduction of ESR when the

concentration of DAT increased, indicating strong secondary interactions between AEMA and DAT in the network, or an effect on the reactivity of the crosslinker in presence of AEMA.

To study the effect of physical interactions between polymer chains, AM-AEMA-BIS-DAT HGs were dried at 37 °C until constant weight, and then swelled again in water for 3 days. Figure 2B shows the values indicated as 1^{st} ESR, corresponding to swelling of the gels equilibrated in water after the synthesis (in which the polymer chains have never been dehydrated), and 2^{nd} ESR, corresponding to dried and re-swollen HGs. During drying, the absence of solvent allows the chains to interact intimately with each other. This approach typically promotes the formation of amorphous and/or crystalline domains, hard to solvate with water. For this reason, the 2^{nd} ESR decreases respect to the 1^{st} ESR for all the samples. In effect, new domains act as pseudo-crosslinks, limiting the access of solvent, and therefore their swelling capacity. It is noteworthy that the decrease in ESR produced by non-covalent interactions is practically independent of DAT concentration. Therefore, the change in ESR upon drying and re-swelling ($\Delta ESR_{RE\text{-}SWELL}$ = 1^{st} $ESR_{AM\text{-}AEMA\text{-}BIS\text{-}DAT}$ - 2^{nd} $ESR_{AM\text{-}AEMA\text{-}BIS\text{-}DAT}$) only shows a small decreasing curve (black squares in Figure 2C), which could be related to a lesser capability to form stable non-covalent domains, due to the reduced chain mobility, promoted by the higher cross-linking degree. The almost DAT-independent ESR diminution observed, indicates that AEMA and DAT do not form particularly strong interactions, which may be expected to be increased in number during the drying and re-swelling process. Therefore, the marked DAT-dependent ESR diminution of AEMA containing HGs, with respect to HGs in absence of AEMA ($\Delta ESR_{AEMA/DAT}$ = $ESR_{AM\text{-}BIS\text{-}}$

DAT - ESR$_{AM-AEMA-BIS-DAT}$, red circles in Figure 2C) could be better related to an increase in the incorporation of DAT as crosslinker (i.e. by reaction of both vinyl ends), when AEMA is present.

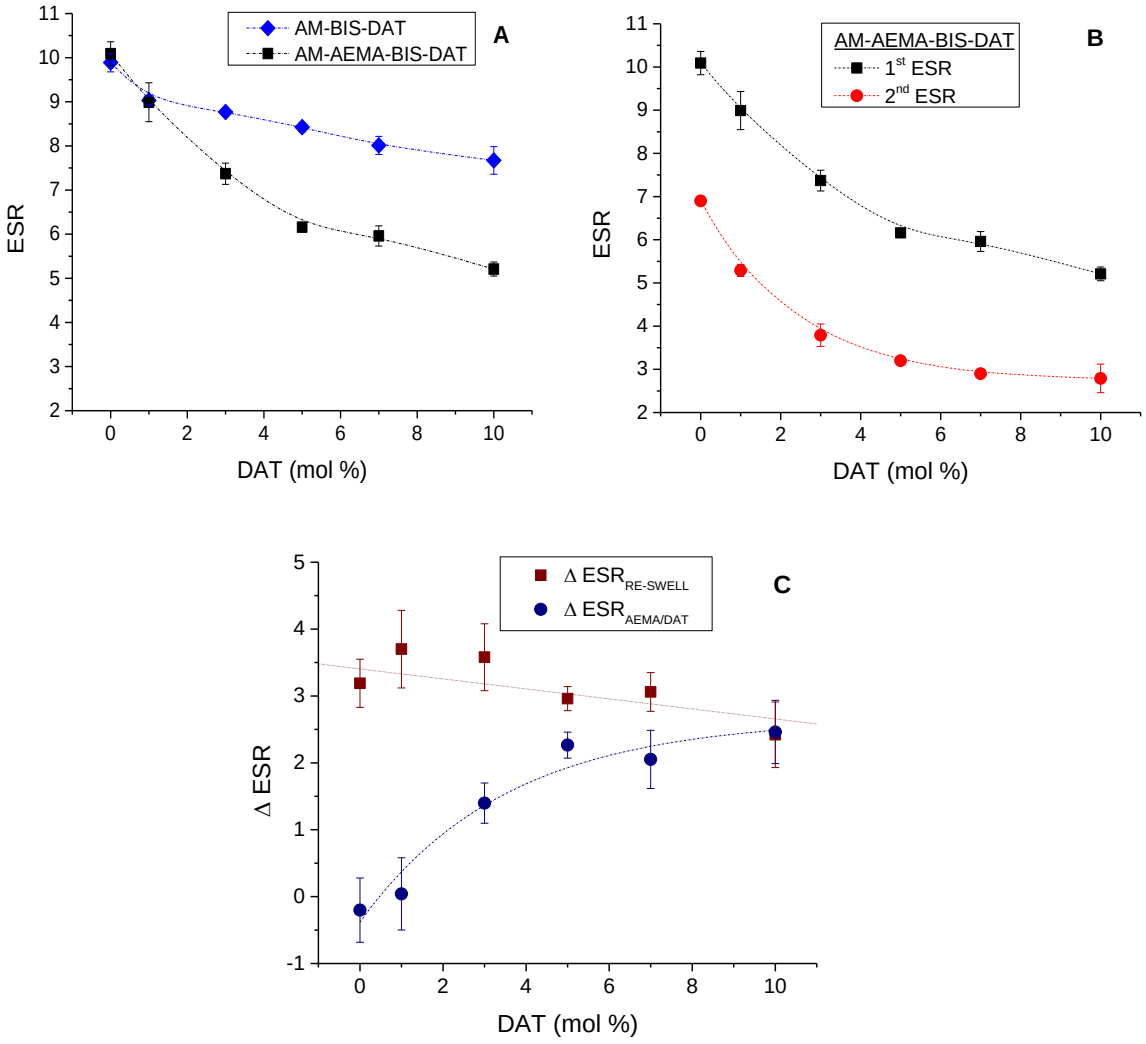

Figure 2.A) Comparison of ESR of HGs, synthesized with (black squares) or without (blue rhombus) AEMA, with respect to %DAT (mol%); B) Dependence on swelling capacity with %DAT after a 1st and 2nd swelling experiment. C) Equilibrium swelling variation (ΔESR) versus %DAT: after consecutive swelling/deswelling experiments in HGs containing AEMA (squares); and between HGs containing AEMA and free of AEMA (circles).

Since HGs will be later treated with aqueous solutions of sodium periodate, understanding how water diffuses into the hydrogels could be useful to interpret how the post-synthesis modification proceeds. For this reason, the swelling kinetics were studied to determine the diffusion mechanism of water into the matrix, and the effect of the percentage of cross-linker used. The swelling kinetic of HGs is closely related to their morphology, to viscous interaction between polymer and solvent, and to polymer-polymer interactions.[38] Except for their morphology, the rest of the characteristics depend on the polymer chemical functionality and cross-linking degree. The swelling rate (SR) over time in p-AM-AEMA-BIS-DAT HGs is shown in Figure 3A. During their swelling, the gels incorporate water quickly at short times, but the swelling rate decreases sharply after reaching 90% of the equilibrium swelling. In general, they reach 50% of the final swelling in approximately 1.5 h, while 95% is achieved in 5 h. This data was used to determine the type of water diffusion mechanism within HGs using Equation 3 (see Materials and Methods). For cylindrical HGs, the theory indicates that: if $0<n<0.5$, the diffusion mechanism of the solvent follows a Fickian behavior, in which only the diffusion rate of the solvent within the matrix is the determinant process; if $0.5<n<1$, it represents a non-Fickian diffusion mechanism in which not only the diffusion of the solvent is relevant, but also the relaxation kinetics of the polymer chains; if $n = 1$, it corresponds to a type II mechanism, in which the swelling kinetic is determined by the speed of relaxation of the chains.[37] The results indicate that the dominant type diffusion of water corresponds to a non-Fickian mechanism in all cases, with values of $n \approx 0.63$, regardless of the degree of cross-linking of the polymers (Figure 3B). These results

confirm that the degree of cross-linking did not affect the relation between water diffusion and chains mobility, despite the previously observed ESR differences.

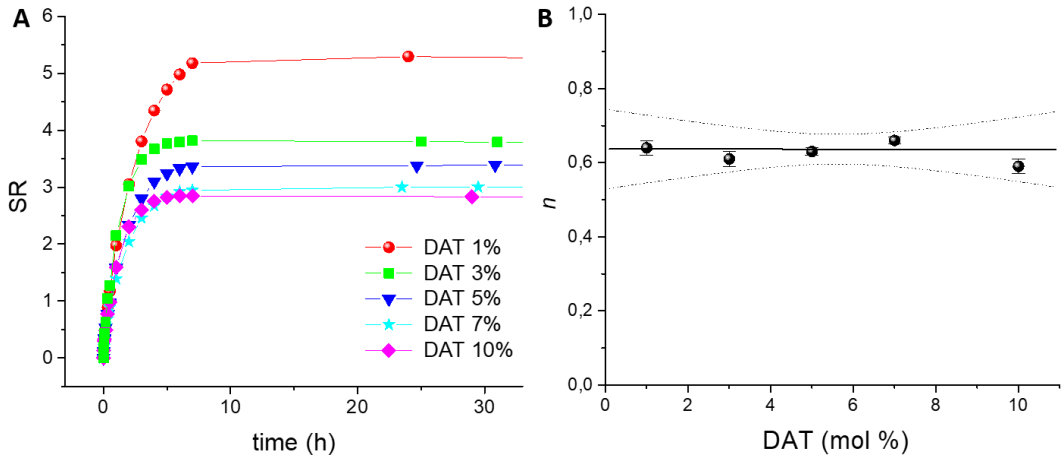

Figure 3. A) Swelling kinetics of p-AM-AEMA-BIS-DAT in water. B) Exponent *n* versus DAT concentration. Straight-line indicate the lineal regression of data and dotted lines shows confidence bands (95%).

Later, the effects caused by the diffusion of periodate into the HGs were studied. For this purpose, fully swollen p-AM-AEMA-BIS-DAT HGs were treated with a sodium periodate solution and changes in swelling rate were followed over time. The changes observed in the swelling rate over time (SR_t) respect to the initial swelling ratio (SR_0) evidenced the cleavage of DAT-crosslinks (Figure 4A and B). In all cases, an increase in the mass and volume of the HGs was observed during the reaction, until reaching a plateau in approximately 5 h. In addition, cross-linked networks with a larger amount of DAT increased the SR up to 40% (see supplementary information, S.I 1). In contrast, networks with low percentage of DAT showed minor increase. When the HG contains

1% DAT (p-AM-AEMA-BIS-DAT(1)) the SR index increased only ≈ 3%. These observations indicate that increasing amounts of DAT where effectively incorporated in the HGs during the synthesis. Moreover, the periodate-mediated cleavage of DAT-crosslinks proceeded selectively, without affecting BIS-crosslinks.

We have previously observed that the periodate cleavage seemed to occur fast, from the outer layers to the core, upon diffusion of the periodate ion into the network.[39] Similarly, Plunkett and collaborators previously reported that the kinetics of periodate-mediated oxidation of glycol pendant groups inside of polymeric hydrogels competed with the diffusion rate of the oxidant into the network, to determine the global kinetics of the reaction. Moreover, they exploited this feature to promote a superficial modification of the HGs.[40] In our case, the kinetic dependence of DAT-cleavage upon periodate diffusion was reflected in the obtained results (see S.I 1). The rate of change of SR with the reaction time showed a clear dependency with the amount of DAT in the HGs. Considering that an excess of periodate was used in all the cases, and that all the networks previously showed a similar diffusion behavior despite their crosslinking degree, the higher rate of change in SR_t/SR_0 observed for HGs with greater amounts of DAT seems to be related to a faster reaction rate caused by a larger amount of DAT-crosslinks in the way of the diffusional front (see S.I 1).

Based on those findings, a kinetic model to correlate the reaction kinetics of diol cleavage with the observed swelling rate changes over time was proposed (see S.I 2). Considering that an excess of periodate was used to perform the cleavage reactions, a pseudo-first order kinetic dependence of the reaction rate with respect to the number of DAT-crosslinks was obtained:

$v = k'.[R_1\text{-DAT-}R_2]$; where $k' = k.[IO_4^{-1}]$ (Equation 4)

Furthermore, considering that the concentration of obtained aldehydes during the reaction is associated with the number of broken DAT-crosslinks, and that both are simultaneously related to the swelling rate of the networks, the following mathematical equation was proposed in order to model the swelling rate changes over time, during the reaction with periodate:

$SR_t = k''.(1 - e^{-k'.t}) + SR_0$ (Equation 5)

Equation 5 was applied to fit the experimental results (figure 4B, dashed line). In summary, the previous observations support the idea that the diffusion of periodate is determinant for the overall reaction rate, while the periodate-mediated cleavage of the diols occurs relatively fast. Since, according to the swelling kinetics experiments, the water diffusion is expected to be similar for all the compositions herein assayed, the cleavage reaction kinetics seems to behave according to a pseudo-first order behavior, with respect to DAT-crosslinks, under the studied reaction conditions.

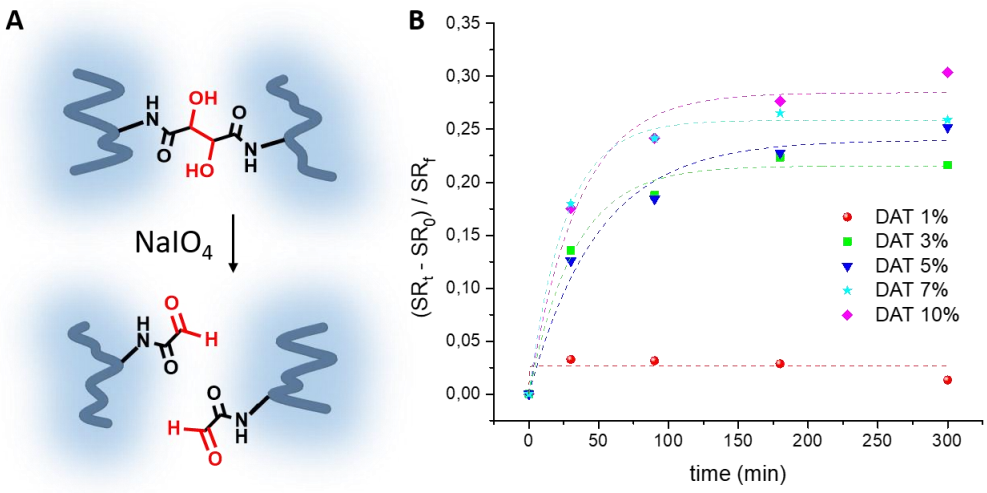

Figure 4 – A) Scheme showing the cleavage of DAT-crosslinks. B) Relative SR index as a function of periodate reaction time for p-AM-AEMA-BIS-DAT HGs. Dotted lines indicate the adjust of data with equation 5.

We have previously reported that the combination of BIS and DAT cross-linking agents enabled the treatment of gels with sodium periodate to generate a selective breakdown of DAT-crosslinks, without affecting BIS-crosslinks, as well as obtaining aldehyde groups into the network.[24] The only way to recover part of the crosslinking points cleaved by periodate was by the external addition of a difunctionalized cross-linker, such as a dihydrazide functionalized molecule, capable of forming covalent bonds with the pendant aldehyde FGs.[24,41] However, in this case, the presence of amino groups, due to AEMA incorporation in the HGs, could enable obtaining self-healing materials based on imine covalent bonds without externally adding a new cross-linker in a subsequent step. To prove this hypothesis, tests were first performed to determine the presence of amines and of α-oxo-aldehyde groups in the HGs, after their treatment with periodate.

Initially, to demonstrate the presence of amine FGs, a chemical test for the reactivity of amines against picryl sulfonic acid (TNBS) was performed. This reagent, which has a yellow color in solution, reacts with primary amine groups to form orange colored compounds, allowing a qualitative visual detection (Figure 5). HGs containing amino (p-AM-AEMA-BIS-DAT(10)) and those without amine groups (p-AM-BIS-DAT(10)) , as well as their respective periodate oxidized products (p-AM-AEMA-BIS-α-oxo-ALD(10) and p-AM-BIS-α-oxo-ALD(10), respectively) were assayed (Figure 5A). The coloration observed after the reaction with TNBS indicated the absence of amino in p-AM-BIS-DAT(10) (negative control) and p-AM-BIS-α-oxo-ALD(10), in which only the typical yellow color of the TNBS solution was observed (Figure 5B, sample 1 and 2, respectively). In contrast, an intense orange color was observed in p-AM-AEMA-BIS-DAT(10) and p-AM-AEMA-BIS-α-oxo-ALD(10) (Figure 5B, samples 3 and 4, respectively), after their reaction with TNBS.

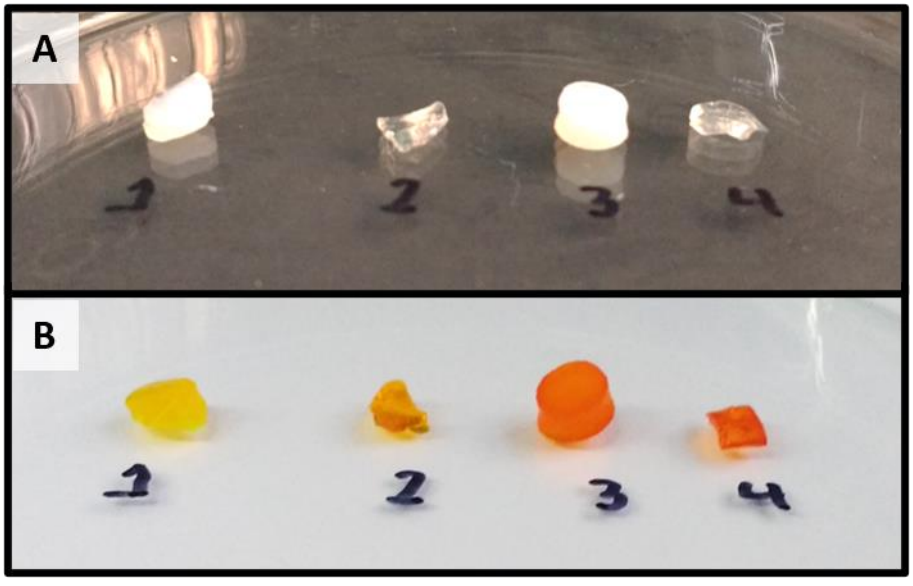

Figure 5 - Identification test of amino groups performed over p-AM-BIS-DAT(10) (1), p-AM-BIS-α-oxo-ALD(10) (2), p-AM-AEMA -BIS-DAT(10) (3), and p-AM-AEMA-BIS-α-oxo-ALD(10) (4); A) Samples before TNBS addition; B) Samples after reaction with TNBS.

Later, an FT-IR study of p-AM-AEMA-BIS-DAT(10) was performed before and after its modification with periodate, and compared with the absorption spectrum of the cross-linking agent DAT. Figure 6 shows the FT-IR spectra of the samples. The signals at 1061 and 1125 cm^{-1} assigned to the C-O stretching in alcohols, and the wide signal between 3650 and 3200 cm^{-1}, characteristic of O-H stretching, are present in both products, indicating the incorporation of the cross-linker. In addition, the signal assigned to the deformation outside the plane of the -CH belonging to DAT vinyl groups (918 cm^{-1}) was not observed in the HGs, denoting the incorporation of the cross-linker into the network. We have previously reported that the rupture of DAT in aqueous medium leads to formation of hydrated aldehyde groups (geminal diol).[24] This, explains the absence of characteristic bands of aldehyde groups in p-AM-AEMA-BIS-α-oxo-ALD (10) spectrum, and the presence of characteristic bands of alcohol groups, after periodate-mediated cleavage of the cross-links. The signals generally observed in amines are overlapped by the absorption bands of other FGs: the stretching of $-NH_2$ (3500 to 3200 cm^{-1}) is in the region of intense absorbance of O-H stretching; the deformation signal of $-NH_2$ (1610 cm^{-1}, absent in DAT but present in both HGs) could correspond to both p-AEMA and p-AM amide. In the same way, the signal corresponding to C=N stretching of imines is generally observed in the region of 1690 to 1520 cm^{-1}, which overlaps with the stretching region of C=O bonds, in which carbonyl groups from AM, AEMA, BIS, DAT or from its oxidation product may be absorbing.

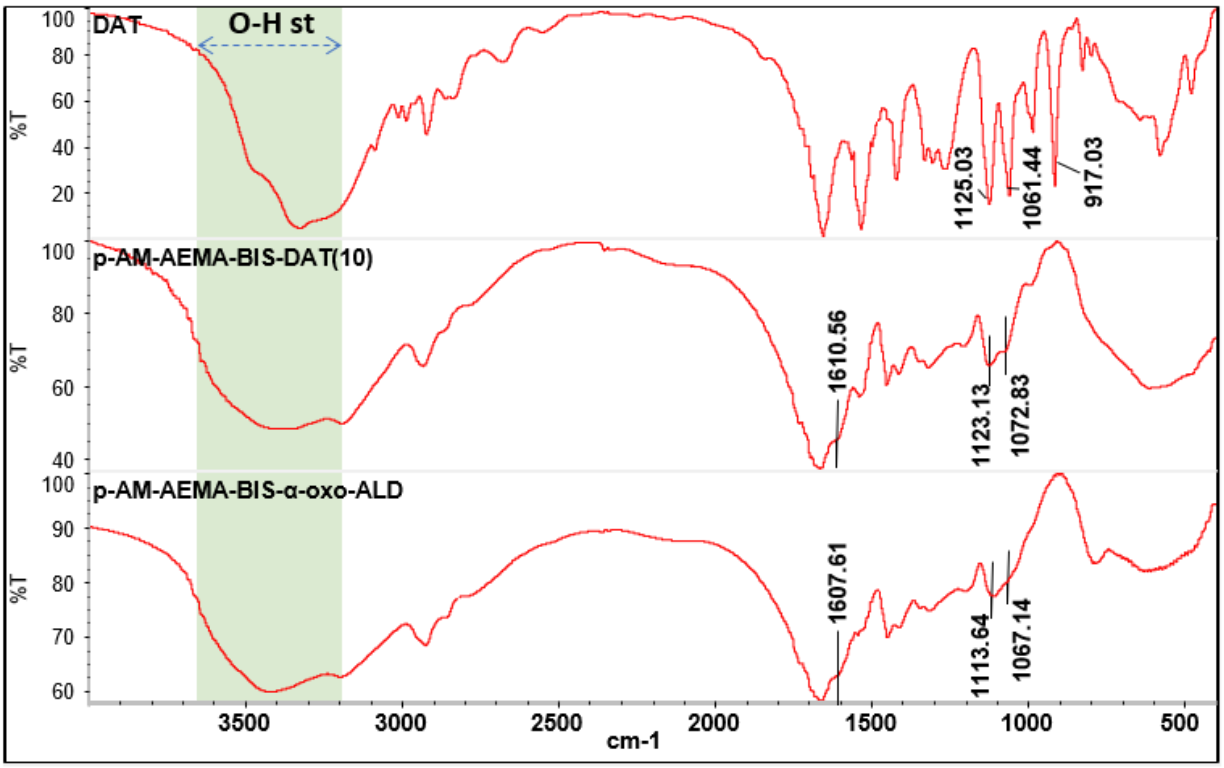

Figure 6 - FT-IR of DAT, p-AM-AEMA-BIS-DAT (10), and p-AM-AEMA-BIS-α-oxo-ALD (10).

p-AM-AEMA-BIS-α-oxo-ALD(10) was then studied by NMR to characterize the chemical nature of polymer network after oxidation with periodate. To perform this procedure, the gel was lyophilized, grinded, and finally rehydrated in D_2O. The ^{1}H-NMR spectrum can be observed in Figure 7. The wide signals are a typical indication of low mobility chains, due to the cross-linked structure of the polymer. However, various signals are clearly distinguished as those of backbone at 1.70 ppm ($-CH_2$) and 2.29 ppm (-CH-) and those belonging to amide ($-NH_2$) of p-AM at 7.09 and 7.82 ppm.[42,43] Furthermore, two small shoulders indicated the presence of aldehydes in the polymeric network: the peak at 5.33 ppm corresponding to the H of hydrated aldehyde group (-C**H**$(OH)_2$), and the signal at 3.23 ppm, providing from the H of methylene, which is adjacent to amide in the aldehyde pendant groups (-C**H$_2$**-NH-R).[24]

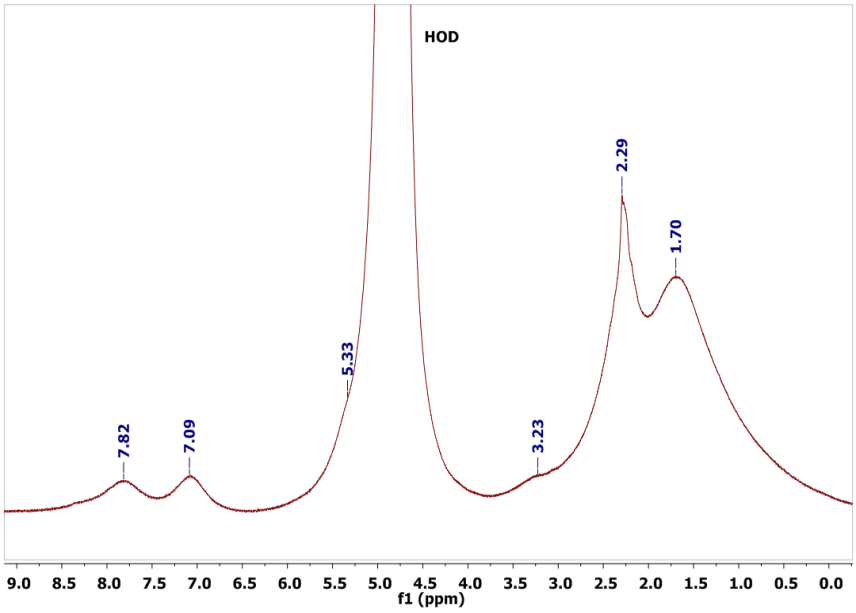

Figure 7 - ^{1}H-NMR spectrum of p-AM-AEMA-BIS-α-oxo-ALD (10) in D_2O.

Moreover, the signals in the ^{13}C spectrum can be more clearly distinguished, due to the C-H decoupling used in the method (Figure 8). The characteristic signals from p-AM backbone (signals *i* and *g* in Figure 8) and amide (signal *a*) are observed.[42] In addition, signals at 87.10 ppm (-**C**H$(OH)_2$) and 172.48 ppm (-NH-**C**(O) -CH$(OH)_2$), indicate the formation of hydrated α-oxo-aldehyde groups, as it has been previously reported for other equivalent molecules.[44] The signals *j* and *e* in the Figure 8 corroborate the incorporation of the AEMA monomer into the polymer network.[45] The low proportion of AEMA monomer used in the synthesis (5% mol) correlates with the low intensity of its signals with respect to others. In addition, the signal of greater intensity in p-AEMA corresponds to its quaternary carbon (*h*), while the others are usually less intense.[45] Moreover, no signals indicating the possible presence of imines (in the range of 150 to 180 ppm) or stable hemiaminals (60 to 90 ppm) were observed.[46] However, this does not imply their absence, but it should be considered that the imines / hemiaminals

formed would be in a low proportion, even less than AEMA, making their detection difficult with this spectroscopic technique.

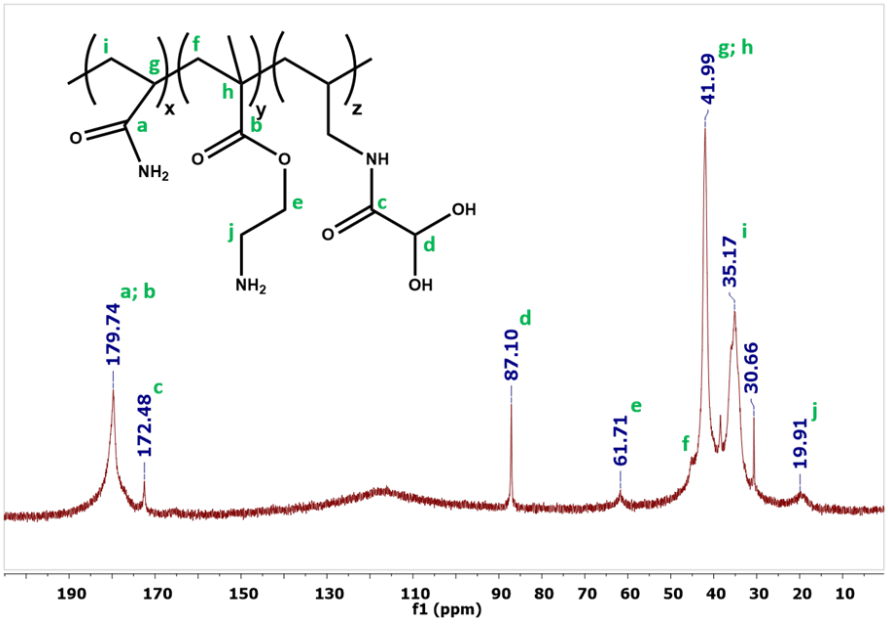

Figure 8 - ^{13}C-NMR spectrum of p-AM-AEMA-BIS-α-oxo-ALD (10) in D_2O.

The AM-BIS-AEMA-DAT HGs demonstrated the formation of amines and α-oxo-aldehydes in the network upon periodate treatment, and were convenient to study how the diffusion of periodate promotes changes in the swelling capacity due to the cleavage of DAT-crosslinks. However, the presence of BIS-crosslinks promotes low mobility of the polymer chains and difficult the formation of imine bonds. For this reason, we next aimed to obtain materials with superior mobility in the polymer chains, to show pronounced smart changes in response to periodate treatment and by imine formation. Consequently, HGs cross-linked only by DAT were synthesized and further studied. For comparison, AEMA-containing HGs (p-AM-AEMA-DAT(10)) and HGs without AEMA (p-AM-DAT(10)) where treated with a solution of sodium periodate. Photographs taken

during the reaction of the HGs against sodium periodate, at different times, are shown in Figure 9. Before starting the reaction, the HGs discs fully swollen in water can be observed (t = 0). After adding a periodate solution, a gradual digestion of HGs was noticed during the first hour of reaction. Meanwhile, the HGs were completely digested to yield viscous liquids. In both cases, the materials remained in a liquid state for at least 8 h. However, as expected, a viscosity increase was observed in p-AM-AEMA-α-oxo-ALD(10).

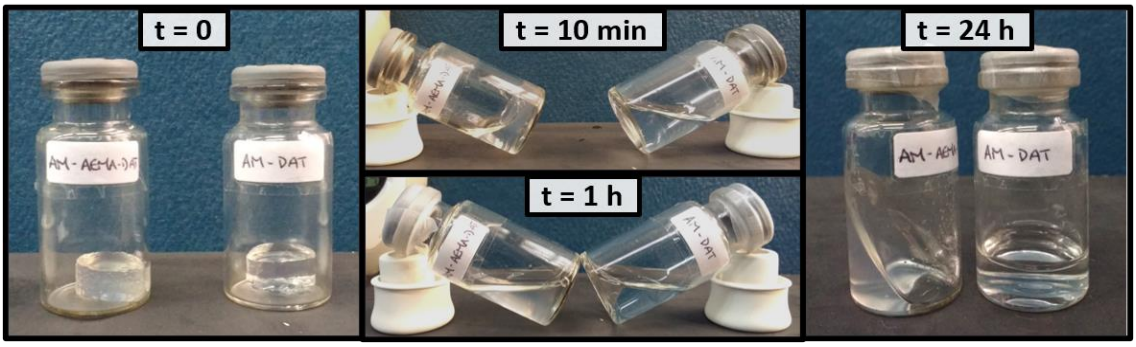

Figure 9. Photographic sequence of cleavage and self-healing in p-AM-AEMA-DAT (glass vial at the left) and its comparison with p-AM-DAT (glass vial at the right).

Finally, after 24 h, the polymer containing amino groups self-healed yielding a new HG, while p-AM-α-oxo-ALD (10) maintained a liquid state. This behavior indicated that the presence of amino and α-oxo-aldehyde groups generates strong imine interactions that led to the reparation of the three-dimensional polymer network (Figure 10).

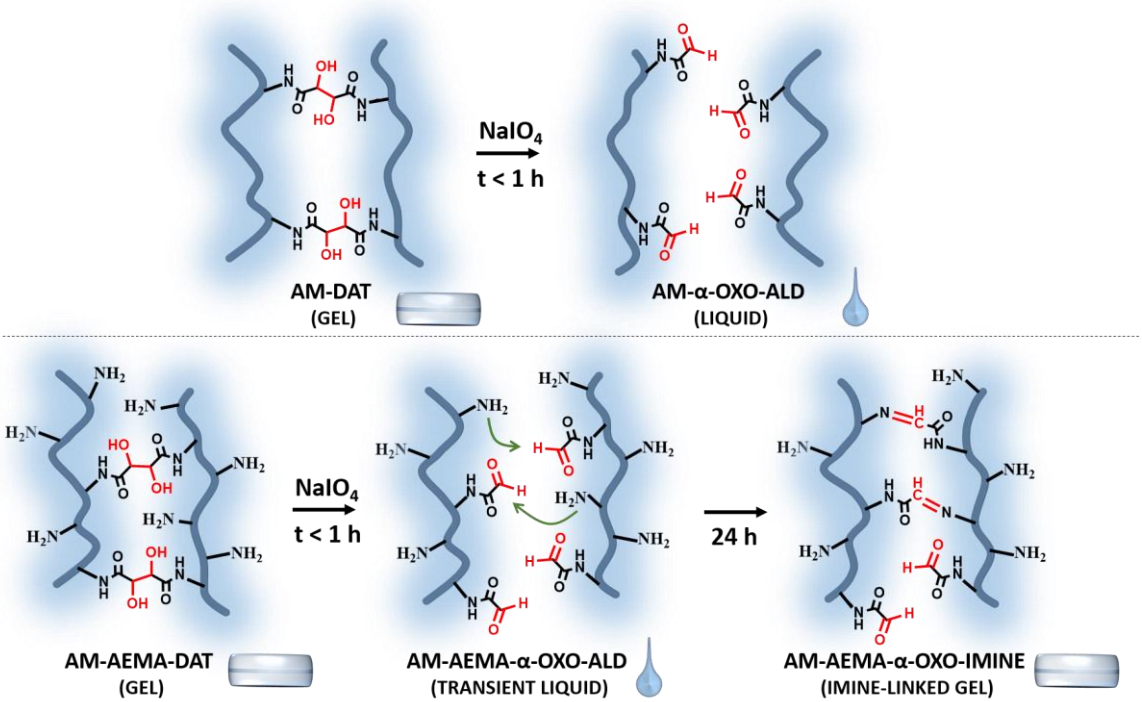

Figure 10) Schematic representation of cross-linking cleavage in p-AM-AEMA-DAT(10) and p-AM-DAT(10) and their evolution over time.

To verify the chemical nature of the interactions in p-AM-AEMA-α-oxo-ALD (10), 0.2 mL of the digested polymer (prior to gelation over time) was diluted in D_2O into an NMR tube and measured after 24 h.

The spectroscopic measurement exhibited a more defined spectrum than the previously obtained in p-AM-AEMA-BIS-α-oxo-ALD(10), given great chain mobility and homogeneity of the sample. In the spectrum (Figure 10) signals due to p-AM are clearly distinguished: H of the backbone at 1.65 and 1.76 ppm (-C**H₂**-); 2.19 and 2.33 ppm (-C**H**-), and H of the amide at 7.82 and 7.09 ppm (-N**H₂**). In addition, signals corresponding to p-AEMA are observed: 1.19 ppm (-C**H₃** attached to main chain) and 3.35 ppm (-C**H₂**-NH_2).

Furthermore, signals at ≈ 5.29 ppm from α-oxo-aldehyde FGs, are present. Part of these aldehyde groups are anchored to the network, evidenced by the signal at 3.21 ppm, corresponding to the methylene adjacent to the amide [-C**H**$_2$-NH-C(O)CH(OH$_2$)]. The other part corresponds to vinyl aldehyde groups, generated after the treatment with periodate from DAT units possibly joined only by one vinyl end to the polymer matrix (signals at 5.86 and 5.21 ppm of vinyl H; signal at 3.85 ppm of the methylene adjacent to the amide).

The reaction of α-oxo-aldehyde with amino FGs to yield imine bonds was evidenced by the appearance of a signal at 7.67 ppm (-C**H**=NH-). This chemical shift is similar to that reported by Hoefnagel and collaborators in the formation of an imine between glyoxylic acid (an α-oxo-aldehyde) and N-methylamine (7.69 ppm).[46]

Therefore, the observations made on the cleavage reactions of p-AM-DAT(10) and p-AM-AEMA-DAT(10) and the subsequent spectroscopic characterization of p-AM-AEMA-α-oxo-ALD(10) demonstrate the formation of imine bonds in the HGs containing amino FGs, triggered by the generation of α-oxo-aldehyde groups by the oxidative cleavage of DAT with sodium periodate.

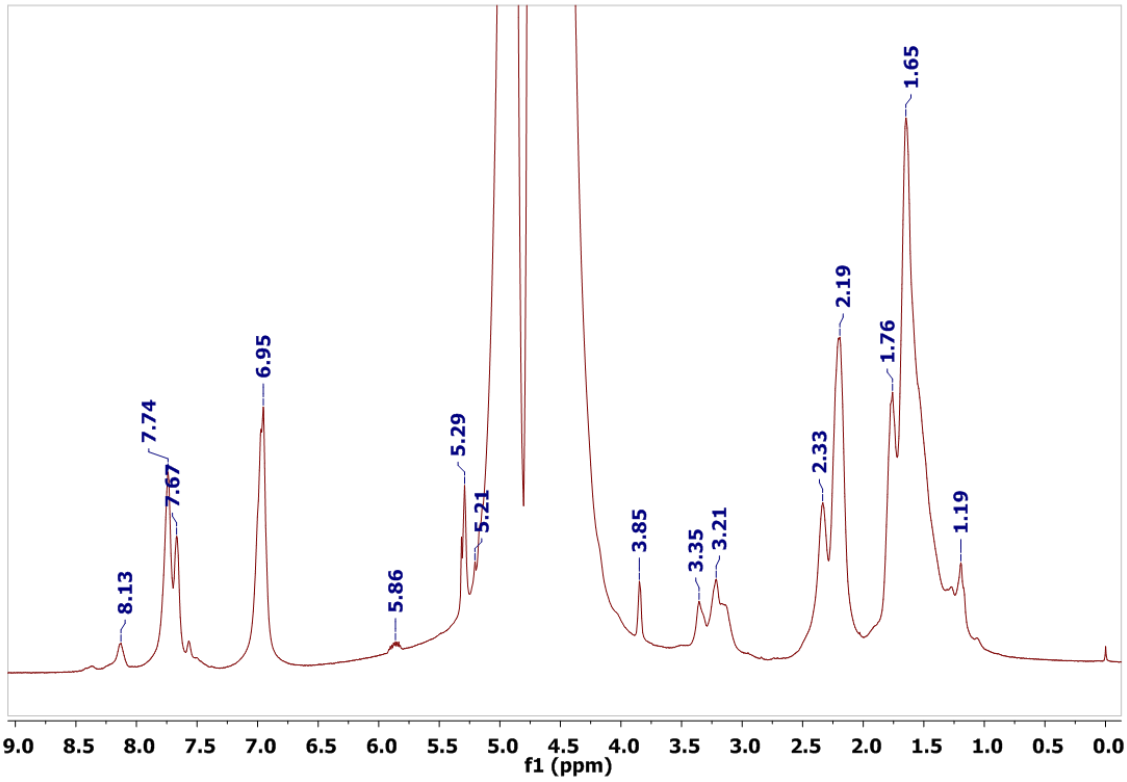

Figure 10 - ^{1}H-NMR of p-AM-AEMA-BIS-α-oxo-ALD(10).

4. CONCLUSIONS

New hydrogels (HGs) based on acrylamide (AM), 2-aminoethyl methacrylate (AEMA) and (+)-*N,N′*-diallyltartardiamide (DAT) as crosslinker, in presence or absence of *N,N′*-methylene bis(acrylamide) (BIS) were developed, envisioning the obtainment of self-healing materials. The studies showed that an increasing incorporation of DAT cross-linker limited the expansion capacity of the network but did not significantly affected water or periodate diffusion. In addition, the use of AEMA seemed to increase the incorporation of DAT, which enlarged the ESR dependency with DAT concentration.

The post-synthetic modification of HGs with sodium periodate solutions caused the selective cleavage of DAT-crosslinks producing changes in the swelling properties.

Moreover, the magnitude and rate of the SR changes showed dependency with the number of DAT-crosslinks present in the network.

The presence of amino FGs in the HGs, together with α-oxo-aldehyde FGs obtained by DAT cleavage, led to the formation of new imine bonds, as it was verified by ^{1}H-NMR. Moreover, it was observed that imine bonds were slowly formed in comparison with oxidative diol cleavage. The combined effect of the kinetics of both reactions enabled the complete break of the HGs structure in presence of periodate, giving a transient liquid material, which later responded giving a self-healed HG at room temperature.

Future studies will focus on the characterization of the kinetic of the gelation process promoted by imine bonds, effects of the density of the involved FGs, the recovery of the mechanical strength, and applications in tissue engineering. In conclusion, the chemical strategy proposed in this work can be applied to design materials with smart properties for specific applications.

5. ACKNOWLEDGMENTS

Authors acknowledge to Consejo Nacional de Investigaciones Científicas y Técnicas (CONICET), Secretaría de Ciencia y Técnica of Universidad Nacional de Córdoba (SECyT-UNC) and Fondo para la Investigación Científica y Tecnológica (FONCyT) for their financial assistance. A. Wolfel thanks CONICET for the endowment of a fellowship.

6. REFERENCES

1. Kamila, S. Introduction, Classification and Applications of Smart Materials: an Overview. *Am. J. Appl. Sci.* **10**, 876–880 (2013).
2. Mahinroosta, M., Jomeh Farsangi, Z., Allahverdi, A. & Shakoori, Z. Hydrogels as

intelligent materials: A brief review of synthesis, properties and applications. *Mater. Today Chem.* **8**, 42–55 (2018).

3. Buwalda, S. J. *et al.* Hydrogels in a historical perspective: From simple networks to smart materials. *J. Control. Release* **190**, 254–273 (2014).

4. Hornat, C. C. & Urban, M. W. Shape memory effects in self-healing polymers. *Prog. Polym. Sci.* **102**, 101208 (2020).

5. Wittmer, A., Wellen, R., Saalwächter, K. & Koschek, K. Moisture-mediated self-healing kinetics and molecular dynamics in modified polyurethane urea polymers. *Polymer (Guildf).* **151**, 125–135 (2018).

6. Krogsgaard, M., Behrens, M. A., Pedersen, J. S. & Birkedal, H. Self-Healing Mussel-Inspired Multi-pH-Responsive Hydrogels. *Biomacromolecules* **14**, 297–301 (2013).

7. Hu, L., Cheng, X. & Zhang, A. A facile method to prepare UV light-triggered self-healing polyphosphazenes. *J. Mater. Sci.* **50**, 2239–2246 (2015).

8. Taylor, D. L. & in het Panhuis, M. Self-Healing Hydrogels. *Adv. Mater.* **28**, 9060–9093 (2016).

9. Mathew, A. P., Uthaman, S., Cho, K. H., Cho, C. S. & Park, I. K. Injectable hydrogels for delivering biotherapeutic molecules. *Int. J. Biol. Macromol.* **110**, 17–29 (2018).

10. Wojtecki, R. J., Meador, M. a & Rowan, S. J. Using the dynamic bond to access macroscopically responsive structurally dynamic polymers. *Nat. Mater.* **10**, 14–27 (2011).

11. Nevejans, S. *et al.* The challenges of obtaining mechanical strength in self-healing polymers containing dynamic covalent bonds. *Polymer (Guildf).* **179**, 121670 (2019).

12. Krishnakumar, B. *et al.* Vitrimers: Associative dynamic covalent adaptive networks in thermoset polymers. *Chem. Eng. J.* **385**, 123820 (2020).

13. Tu, Y. *et al.* Advances in injectable self-healing biomedical hydrogels. *Acta Biomater.* **90**, 1–20 (2019).

14. Imines. *IUPAC Compendium of Chemical Terminology* **2**, 2957 (2014).

15. Belowich, M. E. & Stoddart, J. F. Dynamic imine chemistry. *Chem. Soc. Rev.* **41**, 2003 (2012).
16. Kölmel, D. K. & Kool, E. T. Oximes and Hydrazones in Bioconjugation: Mechanism and Catalysis. *Chem. Rev.* **117**, 10358–10376 (2017).
17. Spears, R. J. & Fascione, M. A. Site-selective incorporation and ligation of protein aldehydes. *Org. Biomol. Chem.* **14**, 7622–7638 (2016).
18. Lei, X., Huang, Y., Liang, S., Zhao, X. & Liu, L. Preparation of highly transparent, room-temperature self-healing and recyclable silicon elastomers based on dynamic imine bond and their ion responsive properties. *Mater. Lett.* **268**, 127598 (2020).
19. Wang, P. *et al.* A self-healing transparent polydimethylsiloxane elastomer based on imine bonds. *Eur. Polym. J.* **123**, 109382 (2020).
20. Liang, R. *et al.* Molecular design, synthesis and biomedical applications of stimuli-responsive shape memory hydrogels. *Eur. Polym. J.* **114**, 380–396 (2019).
21. Gupta, B., Tummalapalli, M., Deopura, B. L. & Alam, M. S. Preparation and characterization of in-situ crosslinked pectin-gelatin hydrogels. *Carbohydr. Polym.* **106**, 312–318 (2014).
22. Han, X., Meng, X., Wu, Z., Wu, Z. & Qi, X. Dynamic imine bond cross-linked self-healing thermosensitive hydrogels for sustained anticancer therapy via intratumoral injection. *Mater. Sci. Eng. C* **93**, 1064–1072 (2018).
23. Negrell, C., Voirin, C., Boutevin, B., Ladmiral, V. & Caillol, S. From monomer synthesis to polymers with pendant aldehyde groups. *Eur. Polym. J.* **109**, 544–563 (2018).
24. Wolfel, A., Romero, M. R. & Alvarez Igarzabal, C. I. Post-synthesis modification of hydrogels. Total and partial rupture of crosslinks: Formation of aldehyde groups and re-crosslinking of cleaved hydrogels. *Polymer (Guildf).* **116**, (2017).
25. Tolvanen, M. & Gahmberg, C. G. In vitro attachment of mono- and oligosaccharides to surface glycoconjugates of intact cells. *J. Biol. Chem.* **261**, 9546–9551 (1986).

26. Norgard, K. E. *et al.* Enhanced interaction of L-selectin with the high endothelial venule ligand via selectively oxidized sialic acids. *Proc. Natl. Acad. Sci. U. S. A.* **90**, 1068–1072 (1993).
27. Zeng, Y., Ramya, T. N. C., Dirksen, A., Dawson, P. E. & Paulson, J. C. High-efficiency labeling of sialylated glycoproteins on living cells. *Nat. Methods* **6**, 207–209 (2009).
28. Kornyšova, O., Jarmalavičiene, R. & Maruška, A. A simplified synthesis of polymeric nonparticulate stationary phases with macrocyclic antibiotic as chiral selector for capillary electrochromatography. *Electrophoresis* **25**, 2825–2829 (2004).
29. Tetala, K. K. R., Chen, B., Visser, G. M. & van Beek, T. a. Single step synthesis of carbohydrate monolithic capillary columns for affinity chromatography of lectins. *J. Sep. Sci.* **30**, 2828–35 (2007).
30. Khaparde, A., Vijayalakshmi, M. A. & Tetala, K. K. R. Preparation and characterization of a Cu (II)-IDA poly HEMA monolith syringe for proteomic applications. *Electrophoresis* **38**, 2981–2984 (2017).
31. Balakrishnan, B. & Jayakrishnan, A. Self-cross-linking biopolymers as injectable in situ forming biodegradable scaffolds. *Biomaterials* **26**, 3941–3951 (2005).
32. Weihang, J., Panus, D., Palumbo, R. N., Tang, R. & Wang, C. Poly(2-aminoethyl methacrylate) with well-defined chain-length for DNA vaccine delivery to dendritic cells. *Biomacromolecules* **12**, 612–626 (2012).
33. Bisht, G., Zaidi, M. G. H. & Kc, B. In vivo Acute Cytotoxicity Study of Poly(2-amino ethyl methacrylate-co-methylene bis-acrylamide) Magnetic Composite Synthesized in Supercritical CO2. *Macromol. Res.* **26**, 581–591 (2018).
34. Chanthaset, N., Ajiro, H., Akashi, M. & Choochottiros, C. A novel comb-shaped polymethacrylate-based copolymers with immobilized 2,4-dihydroxybenzaldehyde for antifungal activity. *Polym. Bull.* **75**, 1349–1363 (2018).
35. Farjadian, F., Schwark, S. & Ulbricht, M. Novel functionalization of porous polypropylene

microfiltration membranes: Via grafted poly(aminoethyl methacrylate) anchored Schiff bases toward membrane adsorbers for metal ions. *Polym. Chem.* **6**, 1584–1593 (2015).

36. Tigges, T., Hoenders, D. & Walther, A. Preparation of Highly Monodisperse Monopatch Particles with Orthogonal Click-Type Functionalization and Biorecognition. *Small* **11**, 4540–4548 (2015).

37. Caykara, T., Kiper, S. & Demirel, G. Thermosensitive poly(N-isopropylacrylamide-co-acrylamide) hydrogels: Synthesis, swelling and interaction with ionic surfactants. *Eur. Polym. J.* **42**, 348–355 (2006).

38. Peters, A. & Candau, S. J. Kinetics of Swelling of Spherical and Cylindrical Gels. *Macromolecules* **21**, 2278–2282 (1988).

39. Wolfel, A., Romero, M. R. & Alvarez Igarzabal, C. I. Post-synthesis modification of hydrogels. Total and partial rupture of crosslinks: Formation of aldehyde groups and re-crosslinking of cleaved hydrogels. *Polymer (Guildf).* **116**, 251–260 (2017).

40. Plunkett, K. N., Chatterjee, A. N., Aluru, N. R. & Moore, J. S. Surface-modified hydrogels for chemoselective bioconjugation. *Macromolecules* **36**, 8846–8852 (2003).

41. Wolfel, A., Romero, M. R. & Alvarez Igarzabal, C. I. Post-synthesis modification of thermo-responsive hydrogels: Hydrazone crosslinking of α-oxoaldehyde obtained from NIPAm-based polymers. *Eur. Polym. J.* **112**, 389–399 (2019).

42. Ziaee, F., Bouhendi, H. & Ziaie, F. NMR study of polyacrylamide tacticity synthesized by precipitated polymerization method. *Iran. Polym. J. (English Ed.* **18**, 947–956 (2009).

43. Bovey, F. A. & Tiers, G. V. D. Polymer NMR spectroscopy. IX. Polyacrylamide and polymethacrylamide in aqueous solution. *J. Polym. Sci. Part A Gen. Pap.* **1**, 849–861 (1963).

44. El-Mahdi, O. & Melnyk, O. α-Oxo Aldehyde or Glyoxylyl Group Chemistry in Peptide Bioconjugation. *Bioconjug. Chem.* **24**, 735–765 (2013).

45. Figueiredo, A. R. P. *et al.* Antimicrobial bacterial cellulose nanocomposites prepared by in

situ polymerization of 2-aminoethyl methacrylate. *Carbohydr. Polym.* **123**, 443–453 (2015).

46. Hoefnagel, A. J., Peters, J. A. & Vanbekkum, H. The Reaction of Glyoxylic Acid with Ammonia Revisited. *J. Org. Chem.* **57**, 3916–3921 (1992).